Sauvain, J. J. ; Rossi, M. J. ; Riediker, M. **Comparison of three acellular tests for assessing the oxidation potential of nanomaterials**. Aerosol Science and Technology, 47(2) :218-227.

Postprint version	Final draft post-refereeing
Journal website	http://www.tandfonline.com/loi/uast20
DOI	10.1080/02786826.2012.742951

Comparison of three acellular tests for assessing the oxidation potential of nanomaterials.

Jean-Jacques Sauvain[1$], Michel J. Rossi[2], Michael Riediker[1]

[1] Institute for Work and Health, Rue du Bugnon 21, CH-1011 Lausanne (Switzerland).

[2] Paul Scherrer Institute, Laboratory of Atmospheric Chemistry (LAC), CH-5232 Villigen PSI (Switzerland).

[$] Corresponding author

Jean-Jacques Sauvain (JJS): jean-jacques.sauvain@hospvd.ch

Tel : ++41 21 314 74 34

Fax : ++41 21 314 74 20

Michel J Rossi (MJR): michel.rossi@psi.ch

Michael Riediker (MR): michael.riediker@hospvd.ch

Abstract:

Great effort is put into developing reliable, predictive, high throughput and low cost screening approaches for the toxicity evaluation of ambient and manufactured nanoparticles (NP). These tests often consider oxidative reactivity, as oxidative stress is a well documented pathway in particle toxicology. Based on a panel of six carbonaceous and five metal/metal oxide (Me/MeOx) nanoparticles, we: i) compared the specifications (linearity, detection limits, repeatability) of three acellular reactivity tests using either dithiothreitol (DTT assay), dichlorofluorescein (DCFH assay) or ascorbic acid (AA-assay) as the reducing agent; and ii) evaluated which physicochemical properties were important for explaining the observed reactivity.

The selected AA assay was found to be neither sensitive nor robust enough to be retained. For the other tests, the surface properties of carbonaceous NP were of utmost importance for explaining their reactivity. In particular, the presence of "strongly reducing" surface functions explained most of its DCFH reactivity and a large part of its DTT reactivity. For the selected Me/MeOx, a different picture emerged. Whereas all particles were able to oxidize DCFH, dissolution and complexation processes could additionally influence the measured reactivity, as observed using the DTT assay.

This study suggests that a combination of the DTT and DCFH assays provides complementary information relative to the quantification of the oxidative capacity of NP.

Keywords

DTT assay; DCFH assay; reactivity tests; surface properties; carbonaceous nanoparticles; metal oxide nanoparticles.

1. Introduction

The induction of oxidative stress by ambient particulate matter (PM) or manufactured nanoparticles (NP) is considered to play a central role in their adverse effects on

human health (Riediker et al., 2004; Foucaud et al., 2007). Oxidative stress results from an imbalance between oxidants and antioxidants. The former are thought to result either from the formation of free radicals by specific constituents of PM (intrinsic oxidative stress) or by activating cells which subsequently release reactive oxygen species (ROS) (Hussain et al., 2009). In this regard, the surface properties are important because it is at this interface that chemical processes or biological interactions take place. The ability of particle surface components (oxidants as well as reducing species) to participate in a redox cycle has been proposed to be a key mechanism for the generation of ROS (Nel et al., 2006). A postulated general mechanism for such redox-cycling is the oxidation of cellular reducing species (glutathione, ascorbic acid,…) by the catalyst (located on the particle), containing kinetically labile oxidation states on its surface. The resulting reduced catalyst is reoxidized by O_2, thereby generating superoxide or hydrogen peroxide (McWhinney et al., 2011).

The risk posed by particles cannot be explained by a single parameter (Bouwmeester et al., 2011). However, the redox properties of PM could be a promising and integrative metric for providing hazard information for risk assessment purposes (Borm et al., 2007), or for decision making through control banding (Grosso et al., 2010). As an enormous manifold of NP is emerging, the use of a conventional toxicological approach as a screening method would be very costly. In this context, acellular tests may prove to be helpful for rapid initial hazard screening, which would subsequently allow researchers to prioritise the different NP to be tested further (by using more specific tests) early during the product development phase. Ayres et al. (2008) reviewed different acellular tests which measure oxidizing substances using electro-physical methods or by measuring the decrease of antioxidants in the presence of particles. Dithiothreitol (DTT), a dithiol compound, shares some similarities with glutathione (Held et al., 1996). The use of DTT has been described for assessing the oxidant potential of ambient PM (Li et al., 2003), of particles collected from Diesel and gasoline engine

exhaust pipes (Geller et al., 2006), the aging process of PM (Li et al, 2009; McWhinney et al., 2011) and also more recently of NP (Sauvain et al., 2008). There are indications that this test has some biological relevance (Li et al., 2003; Steenhof et al., 2011). The dichlorofluorescein assay (DCFH assay) is commonly used for visualising ROS generation at the cellular level but has also been used for determining the intrinsic oxidative potential of NP (Lu et al., 2009). This test takes advantage of the fact that when the reduced form (DCFH) is oxidised, it forms a strongly fluorescent compound (DCF) which can be easily monitored. The sensitivity and the specificity of this test to H_2O_2 is only enabled in the presence of horseradish peroxidase (HRP) (Chen et al., 2010) and some caution regarding the use of this test has been raised (Rota et al., 1999). Nevertheless, the DCFH test has already been used to study the oxidative potency of welding fumes (Antonini et al., 1998) and urban PM (Venkatachari et al., 2005). Another family of acellular tests is based on ascorbic acid (AA) as the reducing species. Bronchoalveolar lavage or synthetic solutions containing AA have been used to characterise the oxidant properties of ambient particles (Mudway et al., 2004), their different fractions (Mudway et al., 2005) and for source apportionment (Godri et al., 2010). More simplified assays have been used to study Diesel particles (Pan et al., 2004). A strong correlation was observed between the acellular oxidant potential of combustion-derived NP toward ascorbic acid and the *in vivo* inflammatory response in mice (Stoeger et al., 2009).

While literature data suggest that at least DTT and AA-based tests could be predictive of biological effects, there has until now been no thorough inter-comparison of these assays. This study intends to fill this gap by evaluating the oxidative potential of a panel of six carbonaceous and five metal/metal oxide (Me/MeOx) NP with DTT, DCFH and an AA-based assay. The repeatability, linearity, and sensitivity of each acellular test will be compared. In addition, we intend to understand which physicochemical properties may be important in explaining the observed reactivity of the NP considered.

2. Materials and methods

2.1. Nanoparticles and chemicals

The NP used in this study (Table 1) were selected based on the following criteria: i. Being representative of some of the most commonly encountered particles in ambient air or in industry; ii. Belonging to the list of proposed reference materials for toxicity tests (Aitken et al., 2008); iii. Providing variability in physicochemical properties; and iv. Being easily commercially available on the scale of hundreds of milligrams.

Table 1

The panel of combustion-generated carbonaceous NP consisted of four carbon blacks (FW2, Printex 90, Printex 60 and FS101, all from Evonik, Germany), representing different surface oxidation levels, and two types of Diesel NP (SRM 2975 and Diesel TPG). The Me/MeOx panel consisted of two types of TiO_2 particles with different anatase to rutile ratios; ZnO and Ag° were studied because of their increasing use in industrial applications and NiO was chosen as a model for highly toxic NP. Because NiO and ZnO can readily dissolve in slightly acidic aqueous solutions, we evaluated the effect of Ni^{2+} and Zn^{2+} ions towards the different reducing species used in the assays. To that end, we used $NiSO_4.6H_2O$ (Sigma Aldrich, Switzerland) and $Zn(CH_3COO)_2.2H_2O$ (Sigma Aldrich, Switzerland) at concentrations ranging between 1-40 µg metal ion/ml. For all tests, particles were suspended in 0.6 mg/L Tween 80® (Fluka, Switzerland). The water used was of highest purity (resistivity > 18.2 MΩ.cm; total organic carbon < 5 ppb) and was produced just before use by a purification system (GenPur, TKA, Hubert, Switzerland). All the other chemicals were of the highest quality available.

2.2. Principles of the DTT, DCFH and AA assays

Three acellular tests were selected: the dithiothreitol (DTT), the dichlorofluorescein (DCFH) and an ascorbic acid-based test (AA test). The oxidant activity of the NP in these three assays is determined by bringing the tested particles into contact with a

reducing chemical (DTT, DCFH or AA) and following either the oxidation of the chemical or the oxygen consumption in solution. Briefly, the reaction rate of the DTT oxidation was determined by measuring the remaining amount of DTT at different reaction times by using a colorimetric measurement following a method described by Sauvain et al. (2008). In the DCFH assay, the presence of oxidising species was assessed from the rapid oxidation of DCFH to the fluorescent DCF species in the presence of HRP, affording low detection levels of H_2O_2. The protocol used is based on the one described by Foucaud et al. (2007). In the AA assay used in this study, the oxidative potential of particles was evaluated by measuring the disappearance of O_2 using an oxygen-specific electrode, as described by Pan et al. (2004).

2.3. Characterisation of NP

The Brunauer-Emmett-Teller (BET) specific surface areas given by the manufacturer were used, if available, otherwise the N_2 adsorption isotherms were determined at the Swiss Federal Institute of Technology in Lausanne (EPFL). The hydrodynamic particle size was determined in a solution containing 0.6 mg/L Tween80® surfactant, as described by Sauvain et al. (2008).

For the combustion-generated NP, organic carbon (OC) and elemental carbon (EC) were determined following the standard NIOSH 5040 procedure (Birch and Carry, 1996) by loading plasma-cleaned and pre-conditioned filter punches (Tissuquartz 2500QAT-UP, Pallflex) with NP. As transition metals have been repeatedly demonstrated to be implicated in oxidative stress/inflammatory processes, we determined the total iron, copper and manganese content of the different carbonaceous NP. The particles were digested in a mixture of 4.9 ml HNO_3 7M and 0.1 ml HF 48%. The resulting solution was analysed by graphite furnace atomic absorption (Perkin-Elmer HGA 700). In addition, we determined the solubility of two metal oxides NP (ZnO and NiO) in the reaction mixture corresponding to the DTT assay. Five ml of the metal oxide suspension (at approximately 120 µg/ml) and 5 ml of the DTT 100 µM were placed in a Vivaspin 15 (5000 MWCO PES, Sartorius) above a 50 ml Falcon tube. After

a 90-minute centrifugation at 4,000 rpm the filtrate was removed. The residue was dissolved in 5 ml acid (HNO_3 7M:HF 48% 49:1 for ZnO and HCl 30%:HNO_3 65% 2:1 for NiO) and centrifuged again for a minimum of 30 minutes at 4,000 rpm. The filtrate and the digested residue were analysed for zinc or nickel content by graphite furnace atomic absorption.

As oxidation-reduction reactions are thought to take place on the particle surface, some of the chemical functions present on the interface of carbonaceous NP were characterised by chemical titration at molecular flow conditions in a Knudsen reactor, as described by Setyan et al. (2009). We used four different gas probes (trimethylamine $N(CH_3)_3$, hydroxylamine NH_2OH, ozone O_3 and nitrogen dioxide NO_2) to titrate different surface functions (online supplemental information, Table S1).

2.4. Statistical evaluation

As the reactivity results can be expressed either in terms of the NP mass or BET surface, both metrics were considered. Pearson correlation coefficients were calculated in order to determine whether there was a statistically significant correlation between different parameters and reactivity. In order to understand the reactivity of the carbonaceous NP with DTT and DCFH tests, we modelled it as a linear combination of the number of reducing, carbonyl and acidic surface functions. Half the values of the LOD were used in the calculations when observables were “not detected”. Calculations were performed using STATA vers.11 software.

3. Results

3.1. Kinetic behaviour and specifications for the three assays

Each NP studied (carbonaceous or Me/MeOx; main characteristics in Table 1) showed linear DTT consumption in the timeframe considered (online supplemental information, Figure S1A for carbonaceous; Figure S1D for Me/MeOx). The reaction rate was thus expressed as nmol of DTT consumed per minute. The reactivity measurements for

Me/MeOx NPs were performed under experimental conditions of excess total metal compared to DTT (molar ratio of total metal to DTT ranged between 1-8.5). The observed DTT oxidation in the presence of NP involves oxygen consumption, as shown clearly for the carbonaceous FW2, Printex 90 and SRM 2975 (online supplemental information, Figure S2), with an experimental stoechiometry of 1.4±0.5 DTT oxidised per O_2 consumed.

For the DCFH assay, we have observed different kinetics depending on the type of particle. After an incubation period of about 30 minutes the increase in fluorescence was quasi-linear as a function of time for most of the carbonaceous NP (online supplemental information, Figure S1B). The reaction rate was therefore expressed as pmol DCF produced/min for the carbonaceous NP. For Me/MeOx NPs, a saturation of the fluorescence signal (for NiO, ZnO and TiO_2 B) or even a decrease of this signal after reaching a maximum (Ag°; TiO_2 A) was observed as a function of time (online supplemental information, Figure S1E and S3). Based on these observations, the kinetics for the DCFH oxidation by Me/MeOx have been approximated by a pseudo-first order rate law by considering the initial 10 minutes of the reaction. The reaction rate was thus expressed as $minutes^{-1}$ for Me/MeOx NP.

The oxygen consumption measured in the AA assay also corresponded to a pseudo-first order rate law and was expressed as $minute^{-1}$ (online supplemental information, Figure S1C). The experiments for Me/MeOx particles were conducted with a molar ratio of total metal to AA comprised between 0.8-1.5 (online supplemental information, Figure S1F).

Table 2 presents the important characteristics of these three assays. The limit of detection (LOD) is defined as the lowest detectable amount of the reactant consumption (DTT, O_2) or formation (DCF) after blank subtraction. It is estimated based on three times the standard deviation of the blank. The DCFH assay was observed to be approximately 10 times more sensitive than the DTT assay. The intrinsic reactivities obtained with the AA assay were smaller than the LOD for all the

NP, except for FW2, Ni^{2+} and Zn^{2+}. For all the studied NP, the DTT assay always showed the smallest coefficient of variation (CV, corresponding to the ratio of the standard deviation to the mean). The linearity domain corresponds to the particle concentration range for which a linear relationship between concentration and reaction rate is observed. Above approximately 8-10 µg/ml of particles in the DTT reacting mixture, an apparent saturating behaviour of the rate change as a function of the particle concentration is observed for Printex 60 and Diesel TPG, possibly indicating agglomeration processes.

Table 2

3.2. Carbonaceous particle characteristics

A linear mass-dependence of the DTT and DCFH reaction rates was observed for all NP, with the slope corresponding to the intrinsic reactivity. Table 3 presents these different intrinsic oxidative reactivities for the panel of NP. The order of reactivity is different depending on the metric used: FW2 was the most reactive based on mass, whereas Diesel TPG appeared to be the most reactive based on surface. When the surface area was considered, all the CBs presented similar values towards DTT (average 195±86 $nmol.min^{-1}.m^{-2}$) and DCFH (average 2.0±0.5 $nmol.min^{-1}.m^{-2}$) whereas this reactivity was larger for Diesel particles (Diesel TPG and SRM 2975). In addition, SRM 2975 was rather reactive toward DTT but did not react at all with DCFH. With the AA assay, oxygen consumption in the presence of ascorbic acid was only detectable with FW2.

Regarding the bulk properties, OC content was very low for the three amorphous CBs as well as for the SRM 2975 sample. For the six carbonaceous NP considered in this panel, OC and EC were negatively associated (r^2: 0.77, $p<0.001$, online supplemental information, Figure S4). The total iron content also increased with the particle OC content, with Diesel TPG presenting the largest amount (online supplemental information, Figure S4). Among the carbonaceous particles, only Diesel TPG presented detectable quantities of copper and manganese (71 and 89 µg/g respectively).

The different surface functions measured using the Knudsen cell technique indicate that FW2, SRM 2975 and Diesel TPG NPs contain between 10 to 100 times more acidic and carbonyl surface functions than the other CBs (Table 3, $N(CH_3)_3$ and NH_2OH gas probe). The sum of "strongly and weakly reducing" surface functions (probed by O_3) was the largest for FS101. Among both Diesel particles, SRM 2975 had about 4-15 times less reducing surface functions (probed by O_3 and NO_2) than Diesel TPG particles.

Table 3

3.3. Correlations between carbonaceous NP characteristics and reactivity

The surface-based as opposed to the mass-based DTT reactivity was significantly and positively associated with OC (r^2: 0.92, $p<0.001$, online supplemental information, Figure S5), but this association was strongly influenced by Diesel TPG. For the studied carbonaceous NP, DTT and particularly DCFH reactivity correlated well with the amount of "strongly reducing" surface groups (probed by NO_2), when either mass (online supplemental information, Figure S6D) or surface-based reactivity (online supplemental information, Figure S7D) were considered. With the O_3 probe, FS101 was clearly an outlier in both assays (online supplemental information, Figure S6C or Figure F7C). When removing this NP, a good association was observed between the number of "strongly and weakly reducing" functions (probed by O_3) and the number of "strongly reducing" functions (probed by NO_2), irrespective of the metric used (mass: $r^2=0.94$, $p<0.001$ or surface: $r^2=0.89$, $p<0.001$).

We tested the association between the mass-based particle reactivity and the particle surface groups (per µg) by calculating reactivity as a linear combination of the independent number of surface functions reacting with NO_2, NH_2OH and $N(CH_3)_3$ (corresponding to "strongly reducing"; "carbonyl" and "acidic" functions respectively). Table 4 shows that all three functional groups were significantly correlated to the mass-based DTT reactivity (adjusted r^2 for the model=0.85, $p<0.001$), whereas regarding the DCFH reactivity, only the number of surface functions reacting with NO_2 was

statistically significant (adjusted r^2=0.77, p<0.001). Similar results were obtained when the surface-based reactivity was used, with the exception that the "acidic" function probed by $N(CH_3)_3$ was no longer significant in the model for DTT reactivity. The constant in the linear combination is not significantly different from zero, which indicates that there is no considerable residual reactivity and that "strongly reducing" and partially oxidized (carbonyl) functional groups seem to explain most of the redox reactivity.

Table 4

3.4. Me/MeOx particle reactivity

Several different reactivity patterns were observed with Me/MeOx NPs. Whereas both types of TiO_2 where not reactive toward DTT (Figure 1A), NiO was associated with a DTT oxidation following a linear mass-dependent function. In contrast, a rate decrease of DTT oxidation was observed in the presence of ZnO compared to a blank (Figure 1A). This rate decrease persisted for reaction mixtures with particle concentrations above ~4 µg/ml. Under our experimental conditions, Ag° presented interesting oxidant effects on DTT, depending on its concentration. Below ~20 µg/ml, the DTT oxidation rate decreased in the presence of Ag° compared to the blank. However, with Ag° concentrations larger than ~20 µg/ml, the DTT oxidation rate exceeded the blank, resulting in the U-shaped reactivity curve in Figure 1A.

Figure 1

All the Me/MeOx NPs studied were able to induce DCFH oxidation at variable levels. Figure 1C suggests that the rate of DCFH oxidation by the studied metallic NP are similar when mass is considered but differed when surface was considered (Figure 1D). This was not observed with the DTT assay. When using the AA assay, all the tested Me/MeOx NPs presented a reactivity below the estimated LOD.

Under our experimental conditions (pH= 7.4), the solubility for ZnO and NiO NPs in the presence of DTT was determined to be 12±2% and 3.4±0.1% respectively. As a consequence, we tested the effect of their ions on reactivity. Zn^{2+} ions exhibited the

same relative rate decrease of DTT oxidation as the particle oxide. On the contrary, Ni^{2+} ions enabled the oxidation of DTT (Figure 1A). In the DCFH assay, these ions were not reactive (Figure 1C). Both Ni^{2+} and Zn^{2+} ions were also able to increase the oxidation rate of AA by oxygen (online supplemental information, Figure S8).

4. Discussion

4.1. Comparison of acellular tests for carbonaceous NP.

Very few data are available to compare our results regarding intrinsic NP reactivity. Nevertheless, our results for Printex 90 and NiO do confirm previous reports that these NP react as oxidants with DCFH (Foucaud et al., 2007; Lu et al., 2009). In addition, the OC and EC contents were comparable to other values in the literature concerning Printex 90 (Stoeger et al., 2009) and SRM 2975 (Singh et al., 2004) as well as for iron in SRM 2975 (Park et al., 2006).

Numerous studies have shown that surface area is an important dose-metric for insoluble particles and that the inflammatory potency of such particles could be the product of the surface area dose times the surface reactivity (Duffin et al., 2007). Regarding their surface chemical functions, the tested CB and Diesel particles possess different functionalities on the same surface, which may even have opposing reactivities (Setyan et al., 2009). The simultaneous presence of both oxidised (probed by NH_2OH or $N(CH_3)_3$), and reducing functions (probed by O_3 or NO_2) (Table 3) may be important when considering particles as a catalyst and could explain the particularly high reactivity observed for some particles (FW2, Diesel TPG). Such a reducing and oxidizing property is central for catalytic activity. The association between DTT or DCFH reactivity and the number of “strongly reducing” surface sites (Table 4 and Figure S6D in online supplemental information) is interpreted as an indication of the ability of the different NP to reduce O_2 on their surface. The oxygen reduction would generate $O_2^{\bullet-}$, and subsequently H_2O_2 through disproportionation. The resulting H_2O_2

would then oxidize either DTT or DCFH (in the presence of horseradish peroxidase). For the DTT assay, this complete catalytic process would correspond to a theoretical stoechiometry of 2 moles of DTT needed for one mole of O_2 consumed. The measured stoechiometry of 1.4±0.5 is in agreement with this mechanism, within experimental error. The importance of the O_2 involvement in the intrinsic oxidative reactivity of NP is further illustrated in Figure S2 (online supplemental information). Surface functions corresponding to such "strongly reducing" sites could be phenoxy radicals (Shiraiwa et al., 2011) or labile hydrogen as in PAH-like structures (Miet et al., 2009; Salgado and Rossi, 2002) or multiply hydroxylated hydroquinones (Stadler, 2000). The fact that we do not observe the same association with "strongly and weakly reducing" functions (probed by O_3, online supplemental information Figure S6C), with FS101 being a clear outlier in both DTT and DCFH assays, could mean that this CB has too few "strongly reducing" functions to generate H_2O_2 in detectable quantities. The additional "weakly reducing" functions would have too low a reduction potential to be able to reduce O_2. The importance of the number of reducing surface groups has recently been highlighted for situations where CB are co-localized with maghemite iron oxide NP (Fe_2O_3) in acidic cellular compartments (Berg et al., 2010). Significant production of oxidants occurred in cells exposed to reduced CB in the presence of Fe_2O_3, but not in cells exposed to a mixture of oxidised CB and Fe_2O_3. In addition, the greater intrinsic redox activity of particles originating from cold-start compared to warm-start wood burning (Miljevic et al., 2010) could be attributable to the larger amount of reducing functions under these particular combustion conditions. Finally, the ability of particles to reduce O_2 may explain the association we found between urinary levels of 8-hydroxydeoxyguanosine (an oxidative stress biomarker) in bus maintenance workers and the sum of "strongly and weakly reducing" functions (reacting with O_3) present on the surface of PM these workers had inhaled (Setyan et al., 2010).

In addition to the "strongly reducing" surface functions, oxidising functions could also participate in the global measured reactivity. As illustrated in Table 4, only the DTT

reactivity is influenced by the presence of carbonyl and possibly acidic surface functions (both considered as potential oxidants). Such carbonyl functions may correspond to quinone or vinylog structures. Indeed, it is known that the DTT assay responds to the presence of quinones (Kumagai et al., 2002). The presence of such redox active organics in the OC fraction could explain the largest surface-based DTT reactivity of Diesel particles compared to CB. The presence of metals could additionally contribute to this reactivity as we observed that Cu° or CuO NP had a quite high oxidant effect towards DTT (unpublished data).

The importance of surface characteristics in modulating the reactivity is exemplified by SRM 2975 and is illustrative of the different specificities of the DTT and DCFH tests. SRM 2975 presents one of the most oxidised surfaces among the panel of carbonaceous NP studied with a low amount of "strongly reducing" sites (Table 3 – NO_2 gas probe). Based on the assumption that "strongly reducing" surface sites are important for reducing O_2 to H_2O_2, it was expected that this Diesel particle would generate a low amount of H_2O_2. Indeed, it was not reactive with the DCFH assay. On the contrary, the observed DTT reactivity would result from the thiol oxidation by the large number of surface carbonyl/acidic functions (Table 3 – NH_2OH or $N(CH_3)_3$ probe). The present data suggest that DCFH and DTT are not responding in an identical manner to the properties of carbonaceous NP. The DCFH assay would respond selectively to the O_2 reduction to H_2O_2 on the particle surface, whereas the DTT assay would in addition respond to the presence of additional oxidized functions such as quinones.

4.2. Comparison of acellular tests for Me/MeOx NP.

Biological injury owing to the presence of NP may also be due to non-oxidant processes as protein interaction (Lynch and Dawson, 2008) or thiol crosslinking (Schrand et al., 2010). The striking difference between the DTT and DCFH assays using Me/MeOx NP relates to the stabilisation effect of ZnO toward DTT oxidation and

the U-shaped curve for Ag° observed also in this assay. Such behaviour was not observed with DCFH (Figure 1).

ZnO is known to be partly soluble in aqueous suspensions depending on pH (Xia et al., 2008). The ZnO solubility of 12±2% measured in this study is in the range of ~10% (at pH 7.2) reported by Song et al. (2010) for similar ZnO NP. Based on the stability constant between Zn^{2+} and DTT (Krezel et al., 2001) and our experimental conditions (ratio $[DTT]/[Zn^{2+}]$ ranging between 1.1 and 24 at pH 7.4), we calculated that all dissolved Zn^{2+} is complexed by DTT. In addition, we cannot rule out the possibility that DTT directly binds to the surface of the remaining ZnO particles. The rather constant stabilisation effect observed above the concentration of ~4 µg/ml ZnO (Figure 1A) may correspond to a situation where only a very small fraction of free (uncomplexed) DTT exists. This complexation process would prevent the formation of the disulfur bond. The stabilisation of DTT toward oxidation in the presence of Zn^{2+} ions has already been reported (Held et al., 1996) and a similar phenomenon has been observed for lead particles collected from a recycling plant (Uzu et al., 2011). The fact that ZnO – but not Zn^{2+} – yields a fluorescent signal with the DCFH probe (Figure 1C) suggests that only ZnO is able to generate ROS in aqueous suspension with O_2. This is an example of the complementary information which may be gathered when using both the DTT and the DCFH acellular assays. Taken together, these results suggest that ZnO may act concomitantly as an oxidant by generating H_2O_2 (or similar ROS; DCFH assay, Appelrot et al., 2009) and as a complexing agent with thiol functions after dissolution (DTT assay). In biological systems, such complexation could remove anti-oxidants (glutathione for example), thereby depriving the cells of a protection mechanism. This is in agreement with the observed cellular toxicity of ZnO NP, which is often attributed to soluble Zn^{2+}, but also to the production of ROS (Xia et al., 2008).

The observed dual mass-dependent DTT reactivity of Ag° could imply a process similar to ZnO. For low Ag° mass concentration (<~20 µg/ml) and in the presence of O_2, Ag^+ ions may be released (Liu and Hurt, 2010) and undergo complexation with DTT. This

complexation will stabilise the DTT toward oxidation as discussed previously for ZnO. This stabilisation could also result from the direct cross-linking of DTT on the surface of Ag° NP, as such processes have been reported for alkane dithiols and Ag° NP in solution (Huda et al., 2010). Above an Ag° concentration of ~20 µg/ml, we postulate that the production of H_2O_2 through dissolution (Liu and Hurt, 2010; Jones et al., 2011) overwhelms the complexation process. This would explain the oxidizing character of silver observed toward DTT. This is in line with the results of the DCFH assay, which also indicates that the system Ag°/Ag^+ acted as an oxidant under our experimental conditions. It is interesting to note that the binding of Ag° to glutathione in addition to its ability to generate ROS *in vitro* has been postulated as one possible mechanism explaining the cytotoxic effect of Ag° NP (Piao et al., 2011).

In the DCFH and DTT assays, NiO NP acted as an oxidizer (Figure 1). This material was shown to generate free radicals in aqueous solutions (Lu et al., 2009). Ni^{2+} ions also showed an oxidant activity with DTT (Figure 1A) and in the AA test (online supplemental information, Figure S8), but not with DCFH. This discrepancy may be owing to the interaction of this ion with HRP, modifying its activity (Mahmoudi et al., 2003). As reported (Shi et al., 1993), the chelation of Ni^{2+}, particularly with thiol functions, is essential for its redox activity. Such complexes can react with O_2 to produce $OH^{\bullet}$ and carbon centered radicals. It was proposed that this activity depends on the ability of the ligand to stabilize Ni^{3+} (Kasprzak et al., 2003). Based on these different acellular reactivity results, we postulate that NiO may act as an oxidant in biological systems by the direct reduction of O_2 on its surface (as suggested by the DCFH assay) and by the dissolution of NiO followed by complexation of Ni^{2+} with thiol functions, rendering it reactive toward O_2 (as suggested by the DTT assay). At a cellular level, such O_2 depletion through Ni^{2+} ions may induce a hypoxic state, which is known to be important for explaining nickel toxicity (Salnikow et al., 2004). In addition, the toxicity of various nickel compounds has been related to their solubility and the bioavailability of Ni^{2+} ions (Forti et al., 2011).

5. Conclusion

By combining the use of DTT, DCFH and AA assays on a panel of six carbonaceous and five Me/MeOx NP, we obtained different, yet complementary results regarding their intrinsic oxidative properties. The reduction of O_2 on the surface of carbonaceous or Me/MeOx NP appears to be an important phenomenon and could be specifically probed by the DCFH assay. The presence of "strongly reducing" functions on the surface of carbonaceous NP was found to be important for explaining both DCFH and DTT oxidizing reactivity. For this last assay, the additional presence of carbonyl surface functions was also important for explaining this reactivity. Furthermore the chemical nature of DTT allows us to detect/mimick potentially biologically relevant oxidative mechanisms induced by NP, like the direct oxidation of thiols (as exemplified for carbonaceous and NiO NP) or their inhibition due to dissolution/complexation to SH functions (as exemplified for ZnO).

As the intrinsic oxidative reactivity of NP appears to be a combination of different processes (reduction of oxygen on their surface, dissolution, and complexation), we propose that a combination of at least the DTT and DCFH assays be used for an initial screening of reactive NP. The importance of these different processes for biological systems should be further evaluated, in order to gain a better understanding of the relationship between NP properties and their *in vitro* and *in vivo* toxicity.

Acknowledgments

We would like to thank Prof. K. Donaldson for the generous gift of the different metal/metal oxide NPs, Dr Aimable for performing the BET measurements of ZnO NP. M. Sanchez-Hohl, S. Deslarzes and N. Gavillet are acknowledged for their excellent laboratory work in measuring reactivity. Thanks also go to C. Kohler for her help in the determination of the metal content in carbonaceous NP and the solubility of ZnO and

NiO. In addition, D. Hart is acknowledged for correcting the English. The French Agence Nationale de Sécurité Sanitaire (ANSES) is acknowledged for its financial support through grant EST 2006/1/7. MJR would like to acknowledge the support of the Swiss National Science Foundation under contract 200020_125204.

References

Aitken, R.J., Hankin, S.M., Tran, C.L., Donaldson, K., Stone, V., Cumpson, P., et al. (2008). A multidisciplinary approach to the identification of reference materials for engineered nanoparticle toxicology. *Nanotoxicology,* 2:71-78.

Antonini, J.M., Clarke, R.W., Murthy, G.G.K., Sreekanthan, P., Jenkins, N., Eagar, T.W., et al. (1998). Freshly generated stainless steel welding fume induces greater lung inflammation in rats as compared to aged fume. *Toxicol. Lett.,* 98:77-86.

Applerot, G., Lipovsky, A., Dror, R., Perkas, N., Nitzan, Y., Lubart, R., et al. (2009). Enhanced antibacterial activity of nanocrystalline ZnO due to increased ROS-mediated cell injury. *Adv. Funct. Mater.,* 19:842-852.

Ayres, J.G., Borm, P., Cassee, F.R., Castranova, V., Donaldson, K., Ghio, A., et al. (2008). Evaluating the toxicity of airborne particulate matter and nanoparticles by measuring oxidative stress potential - A workshop report and consensus statement. *Inhal. Toxicol.,* 20:75-99.

Berg, J.M., Ho, S., Hwang, W., Zebda, R., Cummins, K., Soriaga, M.P., et al. (2010). Internalization of carbon black and maghemite iron oxide nanoparticle mixtures leads to oxidant production. *Chem. Res. Toxicol.,* 23:1874-1882.

Birch, M.E. and Cary, R.A. Elemental carbon-based method for monitoring occupational exposures to particulate Diesel exhaust. *Aerosol Sci. Technol.,* 25:221-241.

Borm, P.J.A., Kelly, F., Kunzli, N., Schins, R.P.F. and Donaldson, K. (2007). Oxidant generation by particulate matter: from biologically effective dose to a promising, novel metric. *Occup. Environ. Med.,* 64:73-74.

Bouwmeester, H., Lynch, I., Marvin, H.J.P., Dawson, K.A., Berges, M., Braguer, D., et al. (2011). Minimal analytical characterization of engineered nanomaterials needed for hazard assessment in biological matrices. *Nanotoxicology,* 5:1-11.

Chen, X., Zhong, Z., Xu, Z., Chen, L. and Wang, Y. (2010). 2',7'-Dichloro-dihydrofluorescein as a fluorescent probe for reactive oxygen species measurement : Forty years of application and controversy. *Free Radical Res.,* 44(6):587-604.

Duffin, R., Tran, L., Brown, D., Stone, V. and Donaldson, K. (2007). Proinflammogenic effects of low-toxicity and metal nanoparticles in vivo and in vitro: Highlighting the role of particle surface area and surface reactivity. *Inhal. Toxicol.,* 19:849-856.

Forti, E., Salovaara, S., Cetin, Y., Bulgheroni, A., Tessadri, R., Jennings, P., et al. (2011). In vitro evaluation of the toxicity induced by nickel soluble and particulate forms in human airway epithelial cells. *Toxicol. in Vitro,* 25:454-461.

Foucaud, L., Wilson, M.R., Brown, D.M. and Stone, V. (2007). Measurement of reactive species production by nanoparticles prepared in biologically relevant media. *Toxicol. Lett.,* 174:1-9.

Geller, M.D., Ntziachristos, L., Mamakos, A., Samaras, Z., Schmitz, D.A., Froines, J.R., et al. (2006). Physicochemical and redox characteristics of particulate matter (PM) emitted from gasoline and Diesel passenger cars. *Atmos. Environ.,* 40:6988-7004.

Godri, K.J., Duggan, S.T., Fuller, G.W., Baker, T., Green, D., Kelly, F.J., et al. (2010). Particulate matter oxidative potential from waste transfer station activity. *Environmental Health Persp.,* 118:493-498.

Groso, A., Petri-Fink, A., Magrez, A., Riediker, M. and Meyer, T. (2010). Management of nanomaterials safety in research environment. *Part. Fibre Toxicol.,* 7:40.

Held, K.D., Sylvester, F.C., Hopcia, K.L. and Biaglow, J.E. (1996). Role of Fenton chemistry in thiol-induced toxicity and apoptosis. *Radiat. Res.,* 145:542-553.

Huda, S., Smoukov, S.K., Nakanishi, H., Kowalczyk, B., Bishop, K. and Grzybowski, B.A. (2010). Antibacterial nanoparticle monolayers prepared on chemically inert surfaces by cooperative electrostatic adsorption (CELA). *ACS Applied Material & Interfaces, 2(4)*, 1206-1210.

Hussain, S.M., Boland, S., Baeza-Squiban, A., Hamel, R., Thomassen, L.C.J., Martens, J.A., et al. (2009). Oxidative stress and proinflammatory effects of carbon black and titanium dioxide nanoparticles: Role of particle surface area and internalized amount. *Toxicology,* 260:142-149.

Jones, A.M., Garg, S., He, D., Pham, A.N. and Waite, T.D. (2011). Superoxide-Mediated Formation and Charging of Silver Nanoparticles. *Environ. Sci. Technol.,* 45:1428-1434.

Kasprzak, K.S., Sunderman, F.W. and Salnikow, K. (2003). Nickel carcinogenesis. *Mutat. Res.,* 533:67-97.

Krezel, A., Lesniak, W., Jezowska-Bojczuk, M., Mlynarz, P., Brasun, J., Kozlowski, H., et al. (2001). Coordination of heavy metals by dithiothreitol, a commonly used thiol group protectant. *J. Inorg. Biochem.,* 84:77-88.

Kumagai, Y., Koide, S., Taguchi, K., Endo, A., Nakai, Y., Yoshikawa, T., et al. (2002). Oxidation of proximal protein sulfhydryls by phenanthraquinone, a component of Diesel exhaust particles. *Chem. Res. Toxicol.,* 15:483-489.

Li, N., Sioutas, C., Cho, A., Schmitz, D., Misra, C., Sempf, J., et al. (2003). Ultrafine particulate pollutants induce oxidative stress and mitochondrial damage. *Environmental Health Persp.,* 111:455-460.

Li, Q.F., Wyatt, A. and Kamens, R.M. (2009). Oxidant generation and toxicity enhancement of aged-Diesel exhaust. *Atmos. Environ.,* 43:1037-1042.

Liu, J.Y. and Hurt, R.H. (2010). Ion release kinetics and particle persistence in aqueous nano-silver colloids. *Environ. Sci. Technol.,* 44:2169-2175.

Lu, S.L., Duffin, R., Poland, C., Daly, P., Murphy, F., Drost, E., et al. (2009). Efficacy of simple short-term in vitro assays for predicting the potential of metal oxide nanoparticles to cause pulmonary inflammation. *Environmental Health Persp.,* 117:241-247.

Lynch, I. and Dawson, K.A. (2008). Protein-nanoparticle interactions. *Nano Today,* 3:40-47.

Mahmoudi, A., Nazari, K., Mohammadian, N. and Moosavi-Movahedi, A.A. (2003). Effect of Mn2+, Co2+, Ni2+ and Cu2+ on horseradish peroxidase. *Appl. Biochem. Biotech.,* 104:81-94.

McWhinney, R.D., Gao, S.S., Zhou, S. and Abbatt, J.P.D. (2011). Evaluation of the effects of ozone oxidation on redox-cycling activity of two-stroke engine exhaust particles. *Environ. Sci. Technol.,* 45:2131 - 2136.

Miet, K., Le Menach, K., Flaud, P.M., Budzinski, H., Villenave, E. (2009). Heterogeneous reactivity of pyrene and 1-nitropyrene with NO_2: Kinetics, products yields and mechanism. *Atmos. Environ.,* 43:837-843.

Miljevic, B., Heringa, M.F., Keller, A., Meyer, N.K., Good, J., Lauber, A,. et al. (2010). Oxidative potential of logwood and pellet burning particles assessed by a novel profluorescent nitroxide probe. *Environ. Sci. Technol.,* 44:6601-6607.

Mudway, I.S., Stenfors, N., Duggan, S.T., Roxborough, H., Zielinski, H., Marklund, S.L., et al. (2004). An in vitro and in vivo investigation of the effects of Diesel exhaust on human airway lining fluid antioxidants. *Arch. Biochem. Biophys.,* 423:200-212.

Mudway, I.S., Duggan, S., Venkataraman, C., Habib, G., Kelly, F. and Grigg, J. (2005). Combustion of dried animal dung as biofuel results in the generation of highly redox active fine particulates. *Part. Fibre Toxicol.,* 2:6.

Nel, A., Xia, T., Madler, L. and Li, N. (2006). Toxic potential of materials at the nanolevel. *Science,* 311:622-627.

Pan, C.J.G., Schmitz, D.A., Cho, A.K., Froines, J. and Fukuto, J.M. (2004). Inherent redox properties of Diesel exhaust particles: Catalysis of the generation of reactive oxygen species by biological reductants. *Toxicol. Sci.,* 81:225-232.

Park, S., Nam, H., Chung, N., Park, J.D. and Lim, Y. (2006). The role of iron in reactive oxygen species generation from Diesel exhaust particles. *Toxicol. in Vitro,* 20:851-857.

Piao, M.J., Kang, K.A., Lee, I.K., Kim, H.S., Kim, S., Choi, J.Y., et al. (2011). Silver nanoparticles induce oxidative cell damage in human liver cells through inhibition of reduced glutathione and induction of mitochondria-involved apoptosis. *Toxicol. Lett.,* 201:92-100.

Riediker, M., Devlin, R.B., Griggs, T.R., Herbst, M.C., Bromberg, P.A., Williams, R.W., et al. (2004). Cardiovascular effects in patrol officers are associated with fine particulate matter from brake wear and engine emissions. *Part. Fibre Toxicol.,* 1:2.

Rota, C., Chignell, C.F. and Mason, R.P. (1999). Evidence for free radical formation during the oxidation of 2'-7'-dichlorofluorescin to the fluorescent dye 2'-7'-dichlorofluorescein by horseradish peroxidase: Possible implications for oxidative stress measurements. *Free Radical Bio. Med.,* 27:873-881.

Salgado, M.S., Rossi, M.J. (2002). Flame soot generated under controlled combustion conditions: heterogeneous reaction of NO_2 on hexane soot. *Int. J. Chem. Kinet.,* 34:620-631.

Salnikow, K., Donald, S.P., Bruick, R.K., Zhitkovich, A., Phang, J.M. and Kasprzak, K.S. (2004). Depletion of intracellular ascorbate by the carcinogenic metals nickel and cobalt results in the induction of hypoxic stress. *J. Biol. Chem.,* 279:40337-40344.

Sauvain, J.J., Deslarzes, S. and Riediker, M. (2008). Nanoparticle reactivity toward dithiothreitol. *Nanotoxicology,* 2:121-129.

Schrand, A.M., Rahman, M.F., Hussain, S.M., Schlager, J.J., Smith, D.A. and Syed, A.F. (2010). Metal-based nanoparticles and their toxicity assessment. *Wires Nanomed. Nanobi.,* 2:544-568.

Setyan, A., Sauvain, J.J., Riediker, M., Guillemin, M. and Rossi, M.J. (2009) Characterization of surface functional groups present on laboratory-generated and ambient aerosol particles by means of heterogeneous titration reactions. *J. Aerosol Sci.,* 40:534-548.

Setyan, A., Sauvain, J.J., Guillemin, M., Riediker, M., Demirdjian, B. and Rossi, M.J. (2010). Probing Functional Groups at the Gas-Aerosol Interface Using Heterogeneous Titration Reactions: A Tool for Predicting Aerosol Health Effects? *Chem. Phys. Chem.,* 11:3823-3835.

Shi, X., Dalal, N.S. and Kasprzak, K.S. (1993). Generation of free-radicals in reactions of Ni(II)-thiol complexes with molecular-oxygen and model lipid hydroperoxides. *J. Inorg. Biochem.,* 50:211-225.

Shiraiwa, M., Sosedova, Y., Rouvière, A., Yang, H., Zhang, Y., Abbatt, J.P.D., Ammann, M., Pöschl, U. (2011). The role of long-lived reactive oxygen intermediates in the reaction of ozone with aerosol particles. *Nat. Chem.,* 3:291-295.

Singh, P., DeMarini, D.M., Dick, C.A.J., Tabor, D.G., Ryan, J.V., Linak, W.P., et al. (2004). Sample characterization of automobile and forklift Diesel exhaust particles and comparative pulmonary toxicity in mice. *Environmental Health Persp.,* 112:820-825.

Song, W.H., Zhang, J.Y., Guo, J., Zhang, J.H., Ding, F., Li, L.Y., et al. (2010). Role of the dissolved zinc ion and reactive oxygen species in cytotoxicity of ZnO nanoparticles. *Toxicol. Lett.,* 199:389-397.

Stadler, D. (2000). A laboratory study of heterogeneous reactions relevant to the atmospheric boundary layer: Soot as a reactive substrate. *Thesis N° 2258*, Ecole Polytechnique Fédérale de Lausanne: Lausanne.

Steenhof, M., Gosens, L., Strak, M., Godri, K.J., Hoek, G., Cassee, F.R., et al. (2011). In vitro toxicity of particulate matter (PM) collected at different sites in the Netherlands is associated with PM composition, size fraction and oxidative potential – the RAPTES project. *Part. Fibre Toxicol.,* 8:26.

Stoeger, T., Takenaka, S., Frankenberger, B., Ritter, B., Karg, E., Maier, K., et al. (2009). Deducing in vivo toxicity of combustion-derived nanoparticles from a cell-free oxidative potency assay and metabolic activation of organic compounds. *Environmental Health Persp.,* 117:54-60.

Uzu, G., Sauvain, J.J., Baeza-Squiban, A., Riediker, M., Sanchez, M., Val, S., et al. (2011). In vitro assessment of the pulmonary toxicity and gastric availability of lead-rich particles from a lead recycling plant. *Environ. Sci. Technol.,* 45:7888-7895.

Venkatachari, P., Hopke, P.K., Grover, B.D. and Eatough D.J. (2005). Measurement of particle-bound reactive oxygen species in Rubidoux aerosols. *J. Atmos. Chem.,* 50:49-58.

Xia, T., Kovochich, M., Liong, M., Madler, L., Gilbert, B., Shi, H.B., et al. (2008). Comparison of the mechanism of toxicity of zinc oxide and cerium oxide nanoparticles based on dissolution and oxidative stress properties. *ACS Nano,* 2:2121-2134.

Figure captions

Figure 1: Relationship between the logarithm of the DTT reaction rate for Me/MeOx relative to the DTT reaction rate in the absence of NP (blank) (k_{MeOx}/k_{blc}) as a function of mass (A) or surface concentration (B). The insert in panel B corresponds to the Ag° NP. Panel C and D represent the DCFH oxidation rate as a function of the mass and surface concentration of Me/MeOx, respectively. The error bars correspond to the uncertainty estimate of the kinetic decay. The dotted line corresponds to the estimated limit of detection for the reaction rate (LOD).

Online supplemental information

Online supplemental information – File presenting additional Table S1 and Figures S1-S8.

Supplemental Information

Comparison of three acellular tests for assessing the oxidation potential of nanomaterials.

Jean-Jacques Sauvain[1], Michel J. Rossi[2], Michael Riediker[1]

[1] Institute for Work and Health, Rue du Bugnon 21, CH-1011 Lausanne (Switzerland).

[2] Paul Scherrer Institute, Laboratory of Atmospheric Chemistry (LAC), CH-5232 Villigen PSI (Switzerland).

1. Gas probes and corresponding surface functions expected to be titrated in the Knudsen cell uptake experiment.

Table S1: Gas-phase probe molecules used to study the surface functional groups of the carbonaceous nanoparticles together with the surface chemical functions they interact with.

Gaseous probe	**Trimethylamine $N(CH_3)_3$**	**Hydroxylamine NH_2OH**	**Ozon O_3**	**Nitrogen dioxide NO_2**
Characteristics of the probe	Base Weak ligand (?)	Oxime formation	Strong oxidant	Radical ; weaker oxidant than O_3
Chemical surface functions probed	Acids (Brönsted/Lewis)	Carbonyls/ Electrophiles	Strongly and weakly reducing functions	Strongly reducing functions
	Ex: - COOH - OH/Lactol	Ex: - C=O (aldehydes, ketones) - Quinones (?)	Ex: - C=C, adsorbed PAH - see NO_2 probe	Ex: - Radicals - Labile hydrogen (Hydroquinones, Polyhydroxyphenols,)

2. Kinetic curves for carbonaceous and Me/MeOx NPs

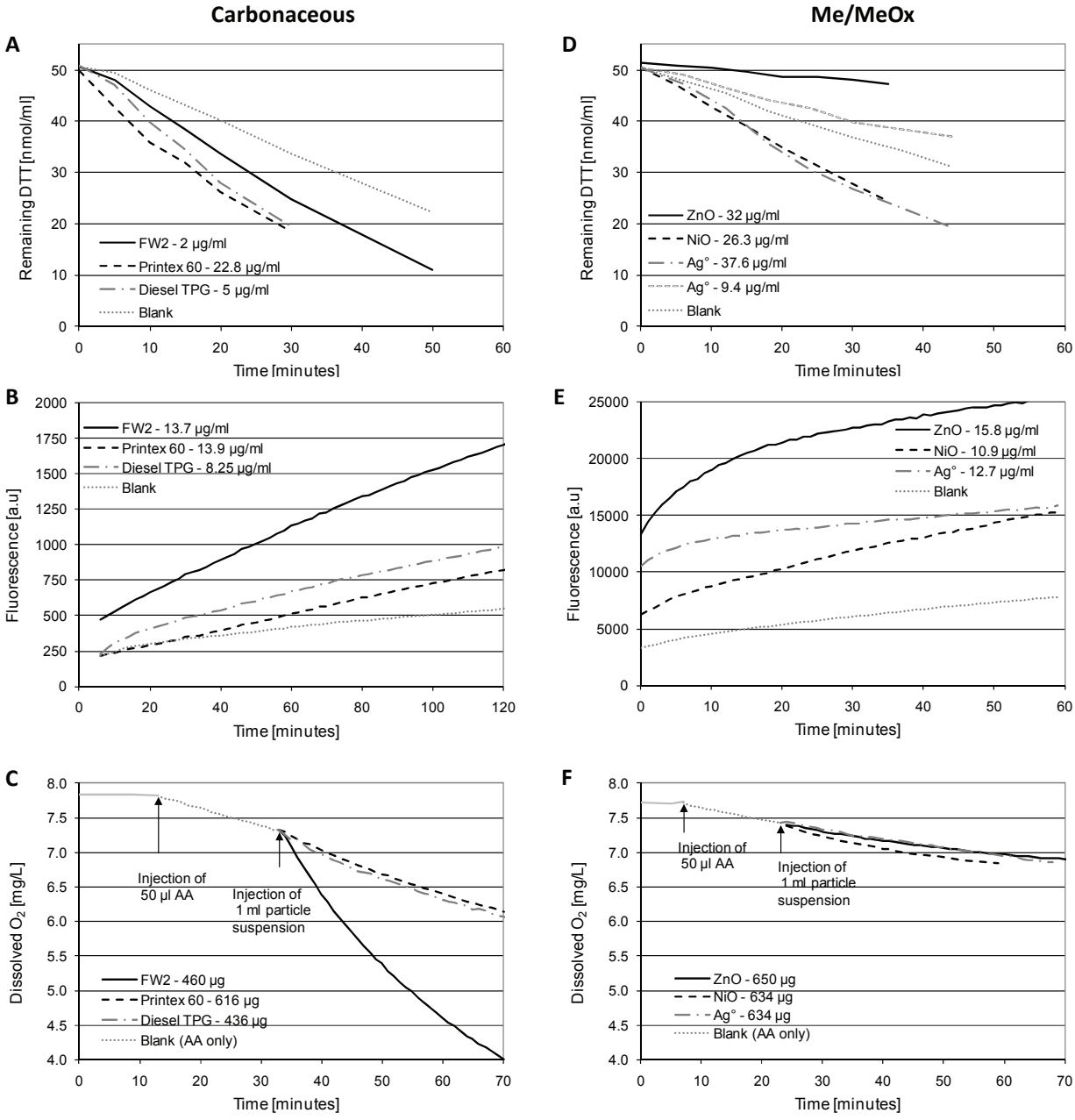

Figure S1: Examples of kinetic curves measured for carbonaceous (panel A-C) and Me/MeOx (panel D-F) nanoparticles in different assays. The particle mass concentration present in the reacting medium is indicated for each test: A) and D) DTT assay; B) and E) DCFH assay; C) and F) Ascorbic acid (AA) assay.

3. Measurement of oxygen consumption in the DTT-CB system

In this experiment, we measured the oxygen consumption when carbonaceous particles are mixed with DTT. The arrows indicate the time when the DTT solution and the particle suspension respectively, were injected into the reactor. For the measurement, we proceeded as described in the protocol for the AA assay (Pan et al., 2004), replacing AA by a DTT solution at a concentration of 28 mM. The final concentrations of the three carbonaceous NPs tested in the reactor are indicated at the bottom of the figure.

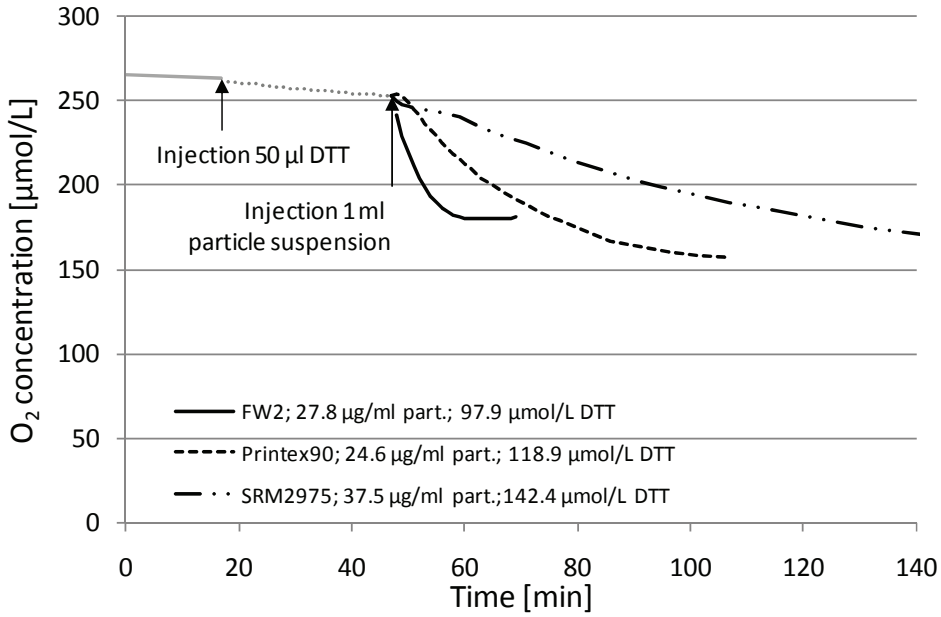

Figure S2: Oxygen consumption in a mixture of DTT and different carbonaceous nanoparticles (FW2; Printex 90 and SRM 2975). Experimental conditions: Phosphate buffer 0.1 M pH 7.4; Tween 80® 0.74 mg/L.

4. Kinetics of the DCFH oxidation by Me/MeOx NP.

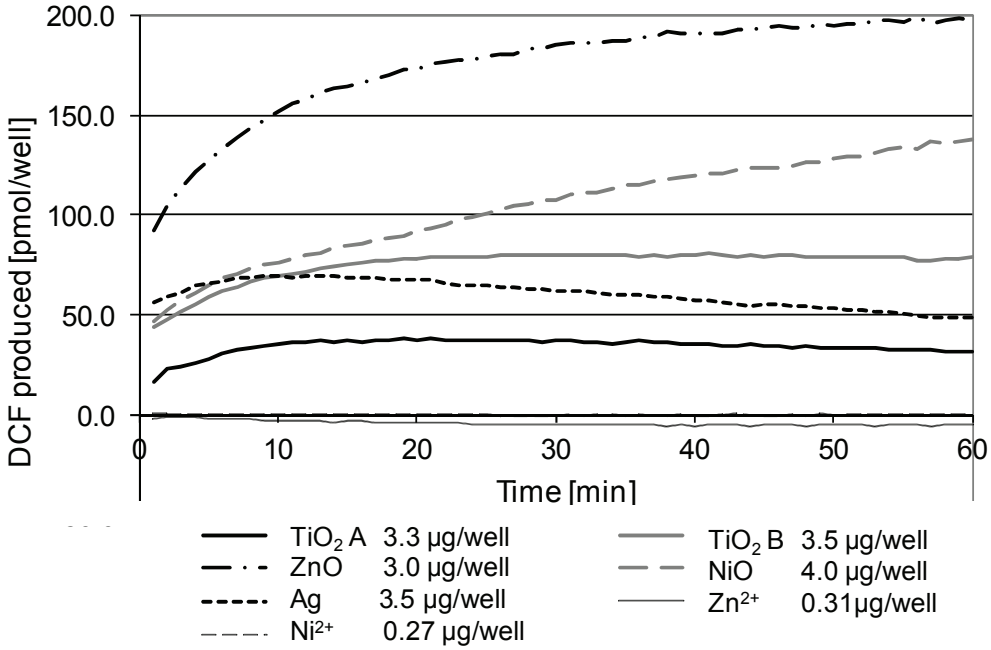

Figure S3: Example of a kinetic trace (blank corrected) for the DCFH oxidation in the presence of Me/MeOx nanoparticles.

The procedure used is described in Foucaud et al., 2007. The final particle mass in each well is indicated below the figure and the final volume of the reacting medium in each well is 0.22 ml.

5. Correlation between the bulk properties of the tested carbonaceous NP.

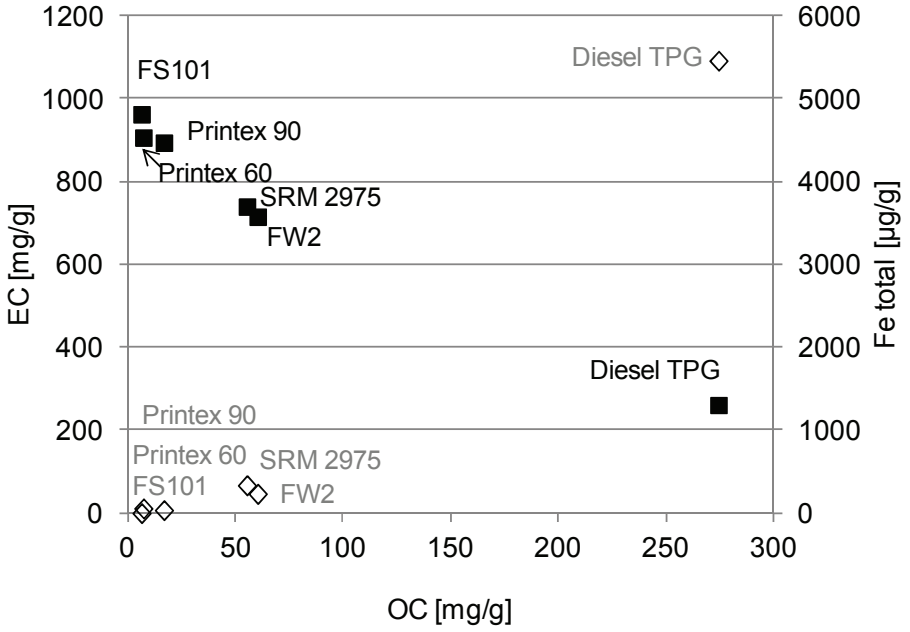

Figure S4: Correlation between the organic carbon (OC) and elemental carbon (EC) content of the various tested carbonaceous nanoparticles (black squares), as well as between OC and Fe (open diamonds).

6. Relationship between the DTT reactivity of carbonaceous nanoparticles and their organic carbon content.

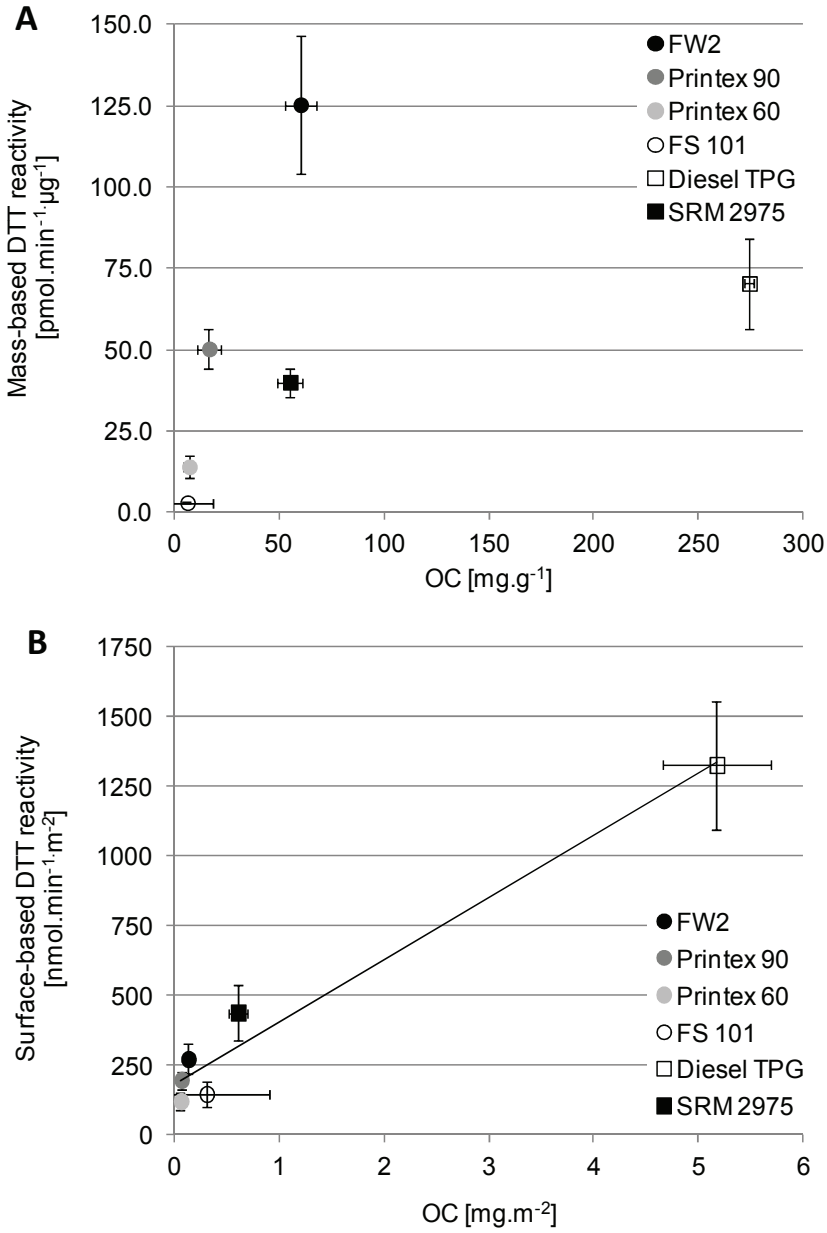

Figure S5: Relationship between the organic carbon (OC) and DTT reactivity based on mass (panel A) or surface area (panel B).

7. Relationship between the reactivity and the surface density of different functional groups on carbonaceous nanoparticles.

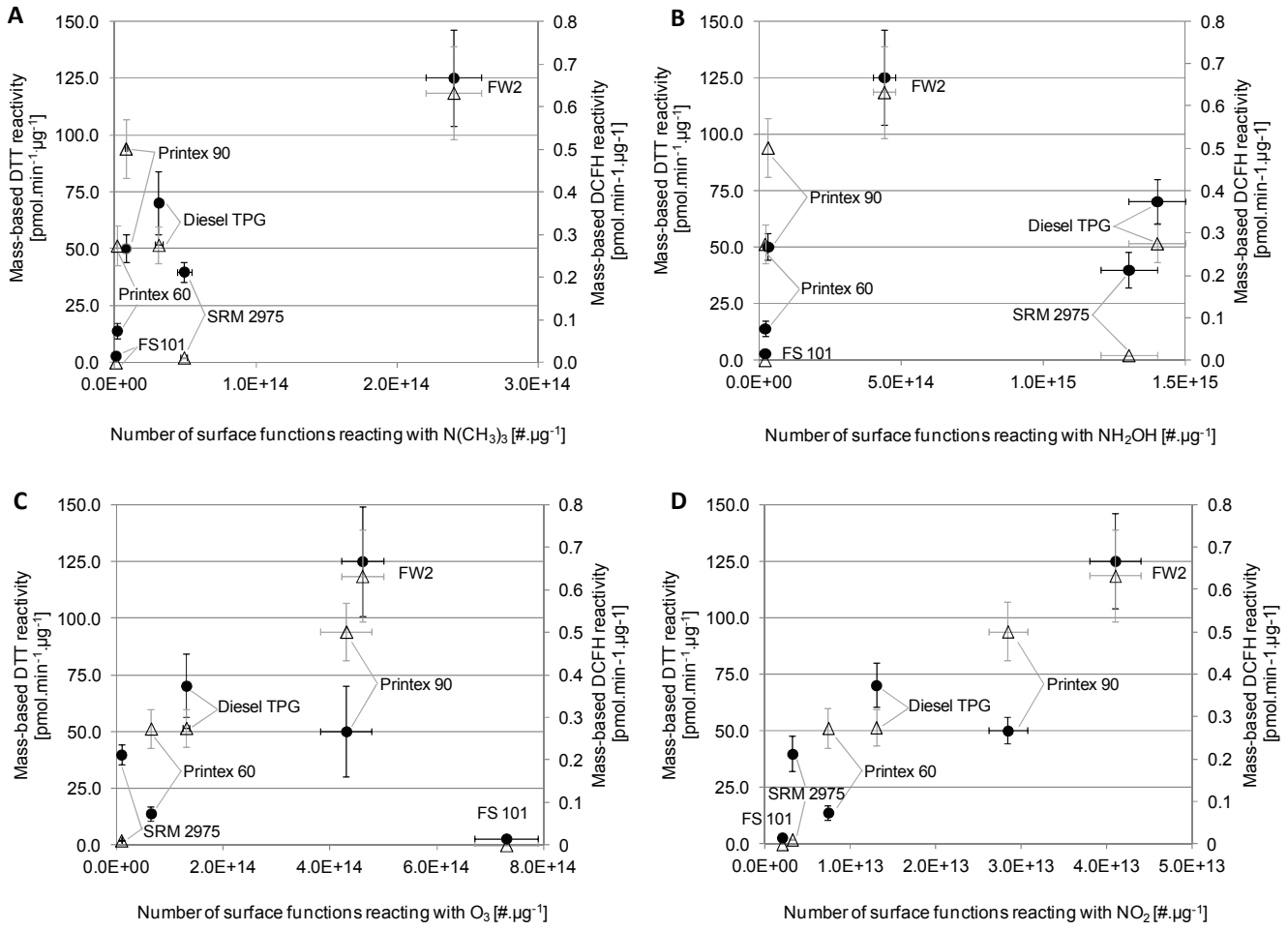

Figure S6: Relationship between the DTT (black dots, left y-axis) or DCFH (open triangles, right y-axis) **mass**-based reactivity of carbonaceous NPs and the number of surface "acidic" (N(CH3)3 probe gas, panel A); "carbonyl" (NH2OH probe gas, panel B); the sum of "strongly and weakly reducing" (O3 probe gas, panel C) or "strongly reducing" only (NO2 gas, panel D) functional groups. The error bars correspond to the propagated uncertainty of each variable.

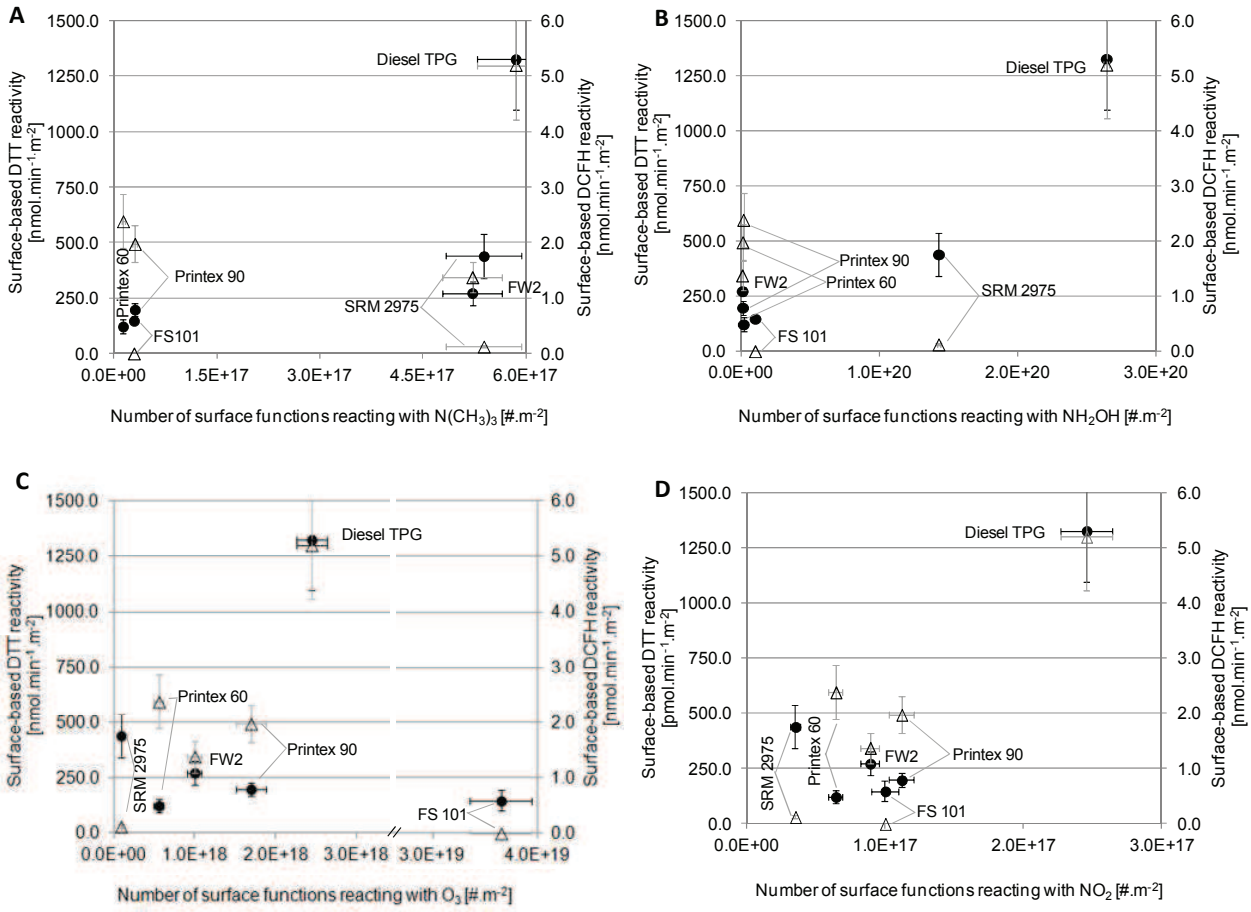

Figure S7: Relationship between the DTT (black dots, left y-axis) or DCFH (open triangles, right y-axis) **surface**-based reactivity of carbonaceous nanoparticles and the surface density of "acidic" ($N(CH_3)_3$ probe gas, panel A); "carbonyl" (NH_2OH probe gas, panel B); the sum of "strongly and weakly reducing" (O_3 probe gas, panel C) or "strongly reducing" (NO_2 probe gas, panel D) functional groups.

8. Oxygen consumption with the ascorbic assay for Ni^{2+}, Zn^{2+} and their corresponding metal oxides.

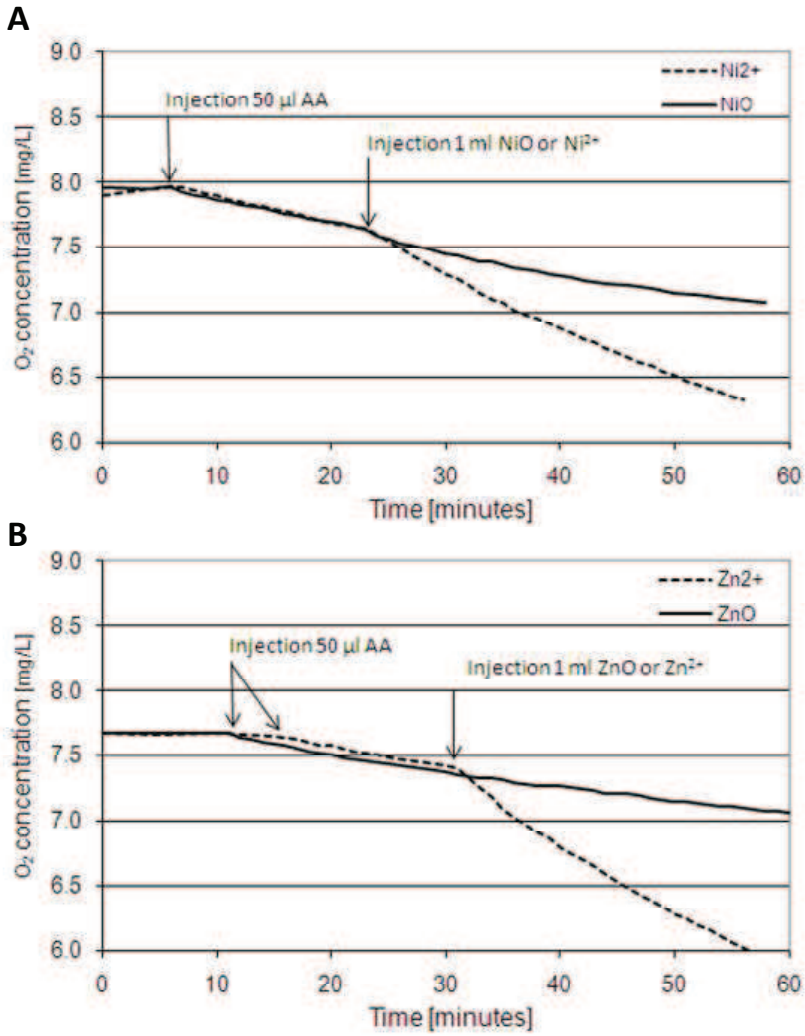

Figure S8: Oxidant effect of the free Ni^{2+} ions (panel A – 189 µg Ni^{2+}/ml) or Zn^{2+} ions (panel B – 239 µg Zn^{2+}/ml) in contrast to the corresponding oxide particulates (NiO – 634 µg NiO/ml; or ZnO – 650 µg ZnO/ml) in the ascorbic assay.

Each arrow indicates the time when the ascorbic acid solution (AA) and the particle/ionic solution respectively, were injected into the reactor. The measurement is performed according to Pan et al., 2004.

9. References

Foucaud, L., Wilson, M.R., Brown, D.M. and Stone, V. (2007). Measurement of reactive species production by nanoparticles prepared in biologically relevant media. *Toxicol. Lett.,* 174:1-9.

Pan, C.J.G., Schmitz, D.A., Cho, A.K., Froines, J. and Fukuto, J.M. (2004). Inherent redox properties of Diesel exhaust particles: Catalysis of the generation of reactive oxygen species by biological reductants. *Toxicol. Sci.,* 81:225-232.

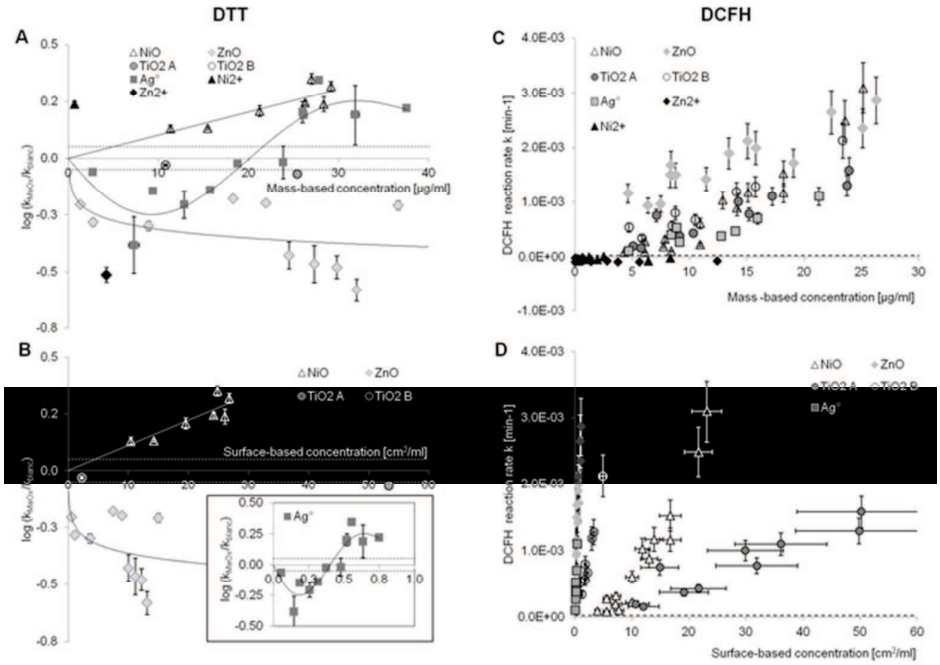

Figure 1: Relationship between the logarithm of the DTT reaction rate for Me/MeOx relative to the DTT reaction rate in the absence of NP (blank) (kMeOx/kblc) as a function of mass (A) or surface concentration (B). The insert in panel B corresponds to the Ag° NP. Panel C and D represent the DCFH oxidation rate as a function of the mass and surface concentration of Me/MeOx, respectively. The error bars correspond to the uncertainty estimate of the kinetic decay. The dotted line corresponds to the estimated limit of detection for the reaction rate (LOD).
58x42mm (300 x 300 DPI)

Table 1: Properties of the nanoparticles used in this study.

Particle	Primary particle size [a] [nm]	BET surface [a] [$m^2.g^{-1}$]	Size distribution of agglomerates [e]			Manufacturer	Remarks
			D10[nm]	D50 [nm]	D90 [nm]		
Carbonaceous							
FW2	13	460	82±3	127±6	204±9	Evonik	
Printex 90	14	254	85±10	150±10	325±10	Evonik	
Printex 60	21	115	104±8	173±11	275±25	Evonik	
FS101	95	20	100±15	176±24	314±51	Evonik	
SRM 2975	29±9[b]	91	89±11	147±16	229±14	NIST	
Diesel TPG	32±10[b]	53[c]	93±9	182±4	324±27	-	Soot retained in a particle trap (Sauvain et al., 2008)
Metal/Metal oxide							
TiO_2 (A)	5-10	210±10	88±2	147±5	256±10	Sigma-Aldrich	99.7% anatase
TiO_2 (B)	60-100	21	107±7	175±11	259±13	Sigma-Aldrich	35% rutile, 65% anatase
NiO	10-20	92	103±13	172±30	272±41	Nanostructural and Amorphous Materials	
ZnO	(a) 20 (b) 415[d]	(a) 50 (b) 4.1[d]	93±12	167±10	266±23	Nanostructural and Amorphous Materials	Important differences between the manufacturer's data (a) and our own measurements (b)
Ag°	85-400	1.5-2.5	264±65	378±60	495±61	Nanostructural and Amorphous Materials	Average particle size quoted as 250-300nm

[a]: Manufacturers' information unless stated otherwise.
[b]: Based on transmission electron microscopy (TEM) measurements done by M. Bonin, Centre de Microscopie de l'Université de Lausanne, Switzerland.
[c]: Brunauer-Emmett-Teller (BET) surface characterisation done by E. Casali, Ecole Polytechnique Fédérale de Lausanne (EPFL), Switzerland.
[d]: TEM and BET characterisation done by A. Aimable, Ecole Polytechnique Fédérale de Lausanne (EPFL), Switzerland.
[e]: in Tween 80® ~0.7 mg/L. D10, D50, D90: 10^{th} , 50^{th} and 90^{th} percentile of the particle diameters determined by Nanoparticle Tracking Analysis.

Table 2: Detection limits (LOD), coefficients of variation (CV) and linearity domain of the three assays used to measure the oxidative potential of carbonaceous or metallic nanoparticles (NP).

Assay	**DTT**	**DCFH**	**AA**
LOD	2.0 $pmol.min^{-1}.\mu g^{-1}$	0.14 $pmol.min^{-1}.\mu g^{-1}$	3.5 $min^{-1}.\mu g^{-1}$
CV carbonaceous NP [%][a]	24 (n=2-16)[b]	29 (n=3-13)	37 (n=3-6)
CV metallic NP [%]	23 (n=2-6)	37 (n=8-15)	- [c]
Linearity domain[d]	0-5 mg/L	0-10 mg/L	0 – 45 mg/L

[a]: for 5 carbonaceous NP, without FS101

[b]: number of repetitions in brackets

[c]: not applicable (all reactivity < LOD)

[d]: corresponding to the particle concentration in the reacting mixture. Determined for carbonaceous NP only.

Table 3: Measured oxidative reactivity, bulk chemical composition (organic carbon - OC, elemental carbon – EC and iron - Fe) and amount of surface functions for the studied carbonaceous nanoparticles.

	FW2	Printex 90	Printex 60	FS101	SRM 2975	Diesel TPG
Oxidative reactivity:						
DTT [pmol/min/µg]	124±29	67±18	11±2	3±1	41±5	73±7
DTT [nmol/min/m^2]	270±78	263±51	98±20	147±64	451±104	1375±315
DCFH [pmol/min/µg]	0.70±0.2	0.50±0.17	0.29±0.06	< 0.14 [b]	< 0.14 [b]	0.28±0.05
DCFH [nmol/min/m^2]	1.5±0.5	2.0±0.8	2.5±0.7	< 7 [b]	<1.5 [b]	5.2±1.5
AA [1E^{-6}/min/µg]	26.3±3.5	< 3.5 [b]	< 3.5 [b]	< 3.5 [b]	< 3.5 [b]	< 3.5 [b]
AA [1E^{-3}/min/m^2]	57±13	< 14 [b]	< 30 [b]	< 175 [b]	< 38 [b]	< 66 [b]
Bulk chemical composition:						
OC [mg/g]	60±8	17±6	7±2	4±9	55±6	274±2
EC [mg/g]	716±12	894±22	907±25	894±132	740±89	261±1
Fe [µg/g]	234	37	58	<2[b]	337	5460
Surface functions probed with:						
$N(CH_3)_3$ [#/mg] [a]	2.4±0.2E+17	7.7±0.7E+15	1.5±0.3E+15	5.8±1.4E+14	4.9±0.5E+16	3.1±0.3E+16
NH_2OH [#/mg] [a]	4.4±0.4E+17	3.1±0.3E+16	< 4.2E+16[b]	< 4.2E+16 [b]	1.3±0.1E+18	1.4±0.1E+18
O_3 [#/mg] [a]	4.6±0.4E+17	4.3±0.5E+17	6.4±0.7E+16	7.3±0.6E+17	8.3±0.7E+15	1.3±0.1E+17
NO_2 [#/mg] [a]	4.1±0.3E+16	2.8±0.2E+16	7.4±0.6E+15	2.0±0.2E+15	3.2±0.3E+15	1.3±0.1E+16

[a]: For surface-based values see Setyan et al., 2010.

[b]: Below the detection limit.

Table 4: Linear combination of the number of different surface functions (expressed as a number/µg) in relationship to the mass-based reactivity.

Reactivity = α[# "strongly reducing" sites] + β[# "carbonyl" sites] + γ[# "acidic" sites] + Constant

Parameter (Probing gas)		**α (NO_2)**	**β (NH_2OH)**	**γ ($N(CH_3)_3$)**	**Constant**	**r^2 of the model**
DTT assay	Coefficient	$(2.0\pm0.5)E^{-12}$	$(2.9\pm0.7)E^{-14}$	$(1.5\pm0.7)E^{-13}$	-4.4±10.2	0.85
	p	0.001	0.001	0.036	0.667	0.001
DCFH assay	Coefficient	$(1.9\pm0.3)E^{-14}$	$(-1.7\pm5.3)E^{-17}$	$(-3.3\pm4.0)E^{-16}$	0.022±0.039	0.77
	p	0.0001	0.751	0.411	0.578	0.001